haematologica
Journal of the Ferrata Storti Foundation

Timing of microbial exposure and risk of infection-promoted acute lymphoblastic leukaemia

by Valeria Cazzaniga, Elham Shamsaei, Julia Proctor, Peter John-Baptiste, Anthony M. Ford and Mel Greaves

Received: September 26, 2025.
Accepted: April 3, 2026.

Citation: Valeria Cazzaniga, Elham Shamsaei, Julia Proctor, Peter John-Baptiste, Anthony M. Ford and Mel Greaves. Timing of microbial exposure and risk of infection-promoted acute lymphoblastic leukaemia. Haematologica. 2026 Apr 16. doi: 10.3324/haematol.2025.289280 [Epub ahead of print]

Letter to the Editor

Timing of microbial exposure and risk of infection-promoted acute lymphoblastic leukaemia

Valeria Cazzaniga*, Elham Shamsaei*, Julia Procter,
Peter John-Baptiste, Anthony M. Ford** and Mel Greaves**

Centre for Evolution and Cancer,
The Institute of Cancer Research,
32 Oakleaf Avenue,
London, SM2 5GP
UK

The datasets used and/or analysed during the current study are available from the corresponding authors on reasonable request.

Word count: 1396

Correspondence

M. Greaves mel.greaves@icr.ac.uk

A. Ford tony.ford@icr.ac.uk

*VC and ES contributed equally as first authors

**AMF and MFG contributed equally as senior authors

Centre for Evolution and Cancer,

The Institute of Cancer Research,

32 Oakleaf Avenue,

London, SM2 5GP

UK

Disclosures

No conflicts of interest to disclose.

Contributions

MG and AMF designed the study and co-wrote the paper. VC, ES, JP and PJ-B carried out the in vivo mouse investigations. ES analysed bacterial 16s and diversity measures. We thank Drs Marco Punta and Sureyya Kose for additional bioinformatic analyses. All authors read and approved the final manuscript.

Funding

The authors are supported by grants from Cancer Research UK (CRM171X), The Children's Cancer and Leukaemia Group UK (CCLGA 2019 02), The Edwards Family Prevent ALL Fund and The Institute of Cancer Research, London.

A multifactorial mechanism has been suggested for the causation of childhood B cell precursor acute lymphoblastic leukaemia (BCP-ALL). This proposes that common infections serve as an indirect trigger for ALL in children carrying an in utero generated and clinically covert pre-malignant clone. But, critically, the model proposes that triggering reflects immune dysregulation and is dependent upon a deficit of microbial exposure and immune network priming in infancy (1). A key premise here is that the naive immune network of infants requires priming, principally by the gut microbiome to insure later immune responses to infections are balanced and chronic inflammation avoided; a concept that has strong experimental support, especially in murine models (2). Preliminary studies suggest that the gut microbiome of newly diagnosed children with BCP- ALL is less mature and diverse than age matched controls (3).

These considerations of causality in ALL have raised the possibility of prevention for the most common subtype of childhood cancer (4, 5). Pursuit of this ambitious goal would benefit from testing the causal roles of microbes in a mouse model of BCP-ALL.

A mouse model of the causal hypothesis would need to test two predictions. First, that common infections can trigger BCP-ALL in a fraction of mice engineered to express a common BCP-ALL initiating lesion i.e. *ETV6::RUNX1*. And, secondly, that this environmental trigger is only effective in the context of a deficit of early life, microbial exposures.

Sanchez-Garcia, Borkhardt and colleagues (6) assessed the first proposition and reported that a fraction (11%) of mice transgenic for *ETV6::RUNX1* or *PAX 5* +/- develop BCP-ALL when transferred from a ‘clean’ housing unit to one (‘dirty’) with endemic microbes, endorsing the idea of infection triggered ALL in susceptible

individuals. We have confirmed this observation. In support of the second proposition, we show that *ETV6::RUNX1* transgenics do not develop ALL if exposed to the same 'leukaemogenic' environment with endemic microbes from birth, or, if transferred to the 'infectious' environment after it was cleared of most endemic microbes by fumigation. All experiments were approved by and conform to the standards of the animal use ethics committee, The Institute of Cancer Research, London, United Kingdom and Home Office license requirements (PPL PP0261348, holder M Greaves).

Figure 1A illustrates the overall incidence levels of ALL in these experiments. BCP-ALL was defined as an expanded population of cells with a B precursor phenotype ($CD19^{+}$, $B220^{+/low}$, IgM^{-}) in blood and bone marrow, clonal *IGH* rearrangement in a clinically sick mouse and, in most cases, an enlarged spleen (Figure 1B, C). A total of 54 mice transferred from a 'clean' to a 'dirty' housing unit between 5 and 8 weeks of age. This time window is earlier than previously reported in a similar mouse model (7) and was chosen because, in mice, microbiome priming of the immune system is most active up until weaning from breast feeding (8). Of those 54 mice, 6 (11%) became sick and were culled (age 14-23m) and had ALL cells as defined above. A further 8 (14.8%) mice were found to have an expanding clonal, BCP population following culling at 24 months and we have assumed they had subclinical ALL (Supplementary Figure 1). One mouse culled at 24 months had a large, clonal T cell (TCRβ) population in addition to a clonal B cell precursor population.

ALL cells would be expected to have genetic alterations that functionally compliment ETV6::RUNX1 (9). We attempted to expand, by transplantation into NSG mice, 3 bone marrow samples of putative ALL diagnosed in mice transferred into the 'dirty' unit. Only one sample regenerated in vivo in sufficient numbers for WGS analysis.

This sample, post-transplant had the same *IGH* rearrangement as the primary sample and, in addition, a deletion in *Ebf1*, and a large deletion on chromosome 10 that included both *Btg1* and *Arid5b* (Supplementary Figure 2A). Also detected in the primary mouse sample by genomic PCR, these deletions are found in diagnostic samples from patients with BCP-ALL and frequently associated with *ETV6-RUNX1* gene fusion (10).

In contrast, no *ETV6::RUNX1* mice (0/400) from a sequential series of cohorts bred and maintained in the 'dirty' facility over a number of years (with sustained endemic infections throughout) developed ALL. Although we did not routinely test for subclinical ALL in these otherwise healthy mice following culling at 24 months, we note that those mice analysed did exhibit polyclonal rearrangements within the *IGH* locus (Supplementary Figure 2B).

When mice bred in the 'clean' facility were transferred into the 'dirty' facility following fumigation and microbial depletion of the latter (following the covid pandemic) no cases of ALL were recorded (0/75) (Supplementary Figure 3A).

We compared the spectrum of microbes present in the 'dirty' facility before (i.e. when associated with ALL) with post fumigation (i.e. in the absence of ALL) and also with the microbes reported to be present in the Spanish facility where BCP-ALL also developed following mouse transfer (7). Only one microbe was present in association with ALL in both 'dirty' facilities in London and Spain – this was murine norovirus (MNV) (Table1). We confirmed by PCR that mice faecal samples were MNV positive during the relevant time period pre covid (Figure 2A). This suggests that MNV should be explored as a candidate agent for triggering ALL in these mouse models. Pinworm was also lost from our 'dirty' facility following fumigation. Although not recorded as present in the Spanish facility, there is evidence that pinworm

exposure can accelerate development of ALL in a different mouse model, where both the initiating and secondary mutations are already present, resulting in a high penetrance of ALL (11). There is no suggestion MNV or pinworm are likely triggers for BCP-ALL in children where respiratory viruses have been implicated by epidemiological studies (1). Nevertheless, a mouse model where ALL could be reproducibly induced by a non-transforming infectious agent would aid the assessment of potential intervention measures.

The causal model of BCP-ALL implicates deficiencies of the gut microbiome in infants (1). In support of this, incidence rates of ALL in a mouse model substantially increased following antibiotic exposure within a 'clean' facility (12).The authors concluded that a dysbiotic microbiome rather than exposure to infections was sufficient to drive the development of BCP-ALL in *Pax5-/-* or *ETV6::RUNX1*+ mice. If correct this would contradict the 2-step causal model proposed for BCP-ALL where epidemiological observations support the idea of an exogenous, microbial trigger (1). We note the antibiotic experiment (12) was not carried out in a germ-free facility and therefore involvement of endemic microbes cannot be ruled out.

We explored the diversity and composition of the gut microbiome by bacterial 16s sequencing in a small number of mice maintained in our 'clean' vs. dirty' vs post fumigation 'dirty' facilities. (Figure 2B). Firstly, and in contrast to Vicente-Dueñas et al (12) the microbiome of our *ETV6::RUNX1* mice was no different in diversity from that in wildtype mice in the same genetic background.

The microbiomes from *ETV6::RUNX1* mice in the 'dirty 'facility were significantly more diverse than in the 'clean' facility or in the 'dirty' facility post fumigation. Mice transferred from the 'clean' to the 'dirty' facility acquired a more diverse gut microbiome (Figure 2B). WGS or shotgun sequencing would be required for detailed

analysis of bacterial species composition, but we note that anti-inflammatory, short-chain fatty acid (SCFA) producing genera, (13) were more numerous in the ‘dirty‘ facility (Supplementary Figure 3B).

All mouse models of human disease have limitations. Mice are genetically uniform with very different developmental time frames, metabolic rates, diets, gut microbiomes and environments compared to humans. Most transgenic models of BCP-ALL have the leukaemia initiating lesion present and expressed in effectively all B lineage cells of the mouse in marked contrast to the rare or clonal ETV6-RUNX1 ‘pre-malignant ‘ cells in children prior to a diagnosis (1). One additional limitation of our and similar mouse models (6, 7) is that the resultant ALL had long latencies and were diagnosed in ageing adults.

Accepting the above caveats, the data provide some support for the proposed causal model of BCP-ALL (1). They confirm that endemic, non-pathological infections may trigger BCP-ALL in genetically susceptible mice. They further suggest the possibility that mice may be protected from infection triggered ALL if exposed to those infections from birth and/or if benefiting from a richer, immune priming, anti-inflammatory gut microbiome. Studies such as these will, hopefully, encourage further exploration of the possible prevention of BCP- ALL, perhaps by microbiome boosting.

References

1. Greaves M. A causal mechanism for childhood acute lymphoblastic leukaemia. Nat Rev Cancer. 2018;18(8):471-484.
2. Hooper LV, Littman DR, Macpherson AJ. Interactions between the microbiota and the immune system. Science. 2012;336(6086):1268-1273.
3. Peppas I, Ford AM, Furness CL, et al. Gut microbiome immaturity and childhood acute lymphoblastic leukaemia. Nat Rev Cancer. 2023;23(8):565-576.
4. Greaves M, Cazzaniga V, Ford A. Can we prevent childhood Leukaemia? Leukemia. 2021;35(5):1258-1264.
5. Hauer J, Fischer U, Borkhardt A. Toward prevention of childhood ALL by early-life immune training. Blood. 2021;138(16):1412-1428.
6. Martín-Lorenzo A, Hauer J, Vicente-Dueñas C, et al. Infection Exposure Is a Causal Factor in B-cell Precursor Acute Lymphoblastic Leukemia as a Result of Inherited Susceptibility. Cancer Discov. 2015;5(12):1328-1343.
7. Rodriguez-Hernandez G, Hauer J, Martin-Lorenzo A, et al. Infection Exposure Promotes ETV6-RUNX1 Precursor B-cell Leukemia via Impaired H3K4 Demethylases. Cancer Res. 2017;77(16):4365-4377.
8. Al Nabhani Z, Dulauroy S, Marques R, et al. A Weaning Reaction to Microbiota Is Required for Resistance to Immunopathologies in the Adult. Immunity. 2019;50(5):1276-1288.e5.
9. Papaemmanuil E, Rapado I, Li Y, et al. RAG-mediated recombination is the predominant driver of oncogenic rearrangement in ETV6-RUNX1 acute lymphoblastic leukemia. Nat Genet. 2014;46(2):116-125.
10. Schwab CJ, Chilton L, Morrison H, et al. Genes commonly deleted in childhood B-cell precursor acute lymphoblastic leukemia: association with cytogenetics and clinical features. Haematologica. 2013;98(7):1081-1088.
11. Fitch BA, Situ J, Wiemels JL, et al. Impact of pinworm infection on the development of murine B-cell leukemia/lymphoma in the presence and absence of ETV6::RUNX1. Haematologica. 2023;108(12):3480-3484.
12. Vicente-Duenas C, Janssen S, Oldenburg M, et al. An intact gut microbiome protects genetically predisposed mice against leukemia. Blood. 2020;136(18):2003-2017.
13. Yang Q, Wang Z, Liu M, et al. Causal Relationship Between Gut Microbiota and Leukemia: Future Perspectives. Oncol Ther. 2024;12(4):663-683.
14. Ford AM, Palmi C, Bueno C, et al. The TEL-AML1 leukemia fusion gene dysregulates the TGF-beta pathway in early B lineage progenitor cells. J Clin Invest. 2009;119(4):826-836.
15. Lefranc M-P. IMGT databases, web resources and tools for immunoglobulin and T cell receptor sequence analysis, http://imgt.cines.fr. Leukemia. 2003;17(1):260-266.

Table 1

Presence of infectious organisms and leukaemia

	LONDON		SALAMANCA [a]
Microorganism	Period 1 ALL+ (pre fumigation)	Period 2 ALL- (post fumigation)	ALL+
BACTERIA .sp			
Helicobacter sp.	+	+	+
P.pneumotropica-HeyL	+	+	-
P.pneumotropica-Jawetz	+	+	-
P.mirabilis *	+	-	-
Campylobacter sp *	+	-	-
S.aureus *	+	+	-
K.oxytoca *	+	-	-
Aspiriculus tetraptera *	+	-	-
VIRUSES			
MHV *	-	-	+
MNV (Norovirus)	+	-	+
PARASITIC sp			
Pinworm	+	-	-
Trichomonas	+	+	+
S.muris *	+	-	-
Demodex sp (mites) *	+	-	-
E.histolytica *	+	-	-

a: see reference (7)
* Sporadic presence (other organisms are endemic)

FIGURE LEGENDS

Figure 1. Leukaemia in *ETV6::RUNX1* mice transferred from a SPF-1 to SPF-2 facility.

A) Cartoon to show the setup and incidence of ALL for the 'housing switch' model for *ETV6::RUNX1*+ mice (B6CBA) kept under conditions of SPF-1 (clean) or SPF-2 (dirty) or switched from SPF-1 to SPF-2 (top panel). A similar protocol was followed post-fumigation of the SPF-2 facility (bottom panel). The *ETV6::RUNX1* transgene was driven by the human β-globin promoter and lymphoid lineage specificity achieved via the immunoglobulin (*IGH*) heavy chain enhancer (14).

B) Immunophenotype and respective spleen size of a representative *ETV6::RUNX1*+ mouse with ALL. A wild type (WT) and a healthy *ETV6::RUNX1*+ mouse are shown for comparison. The B220 v CD19 FACS plots identify the B-lineage populations and the expanded CD19+/IgM- population of the leukaemic mouse confirms the presence of a B-lineage precursor clone ($CD19^{+}$, $B220^{+/low}$, IgM^{-}). The average spleen size of WT and polyclonal *ETV6::RUNX1*+ mice was 1.6 ± 0.2 cm. The average spleen size of *ETV6::RUNX1*+ mice with *IGH* clonal ALL was 2.0 ± 0.6 cm.

C) DNA sequence of a clonal *IGH* gene rearrangement in BCP from a typical *ETV6::RUNX1*+ mouse with overt leukaemia. Case-specific random nucleotide insertion (*N1, N2*) occurs between the respective V, D and JH joins (15). (All mice with phenotypic BCP-ALL displayed an identical clonal *VNDNJ* rearrangement in both the bone marrow and spleen).

Figure 2. Gut microbiota in SPF-1 and SPF-2 facilities pre- and post-fumigation

A) Presence of MNV in mouse stools pre-fumigation of SPF-2 facility. SYBR green PCR Melt Curves to detect the presence of MNV in cDNA prepared from individual mouse stools collected from the SPF-2 facility at two different time points. Where "-d(RFU)" is the change in fluorescence and "dT" is the change in temperature. The orange trace (Period 1) shows two stools collected in 2018, pre-fumigation; the green trace (Period 2) shows two stools collected in the post covid period (2024) and post fumigation. The thin blue trace is a water control.

B) Shannon diversity index of gut microbiota across genotypes and facility environments. All mice were 8-9 weeks of age. Boxplots represent Shannon entropy values for commercially sourced wild-type mice (**WT-Shop**) compared to facility-raised transgenic (**TG**) and wild-type (**WT**) cohorts. Facility groups are categorized by fumigation status: **Pre-fumigation** (TG-SPF1, TG-SPF2, TG-SPF1-SPF2) and **Post-fumigation** (TG-SPF2, WT-SPF2). The WT-Shop group exhibited significantly higher microbial diversity compared to all facility-born groups (Kruskal–Wallis $P = 0.01$), with all pairwise comparisons against WT-Shop showing significance ($P < 0.05$). Data are presented as box-and-whisker plots,; $n = 3$ per group.

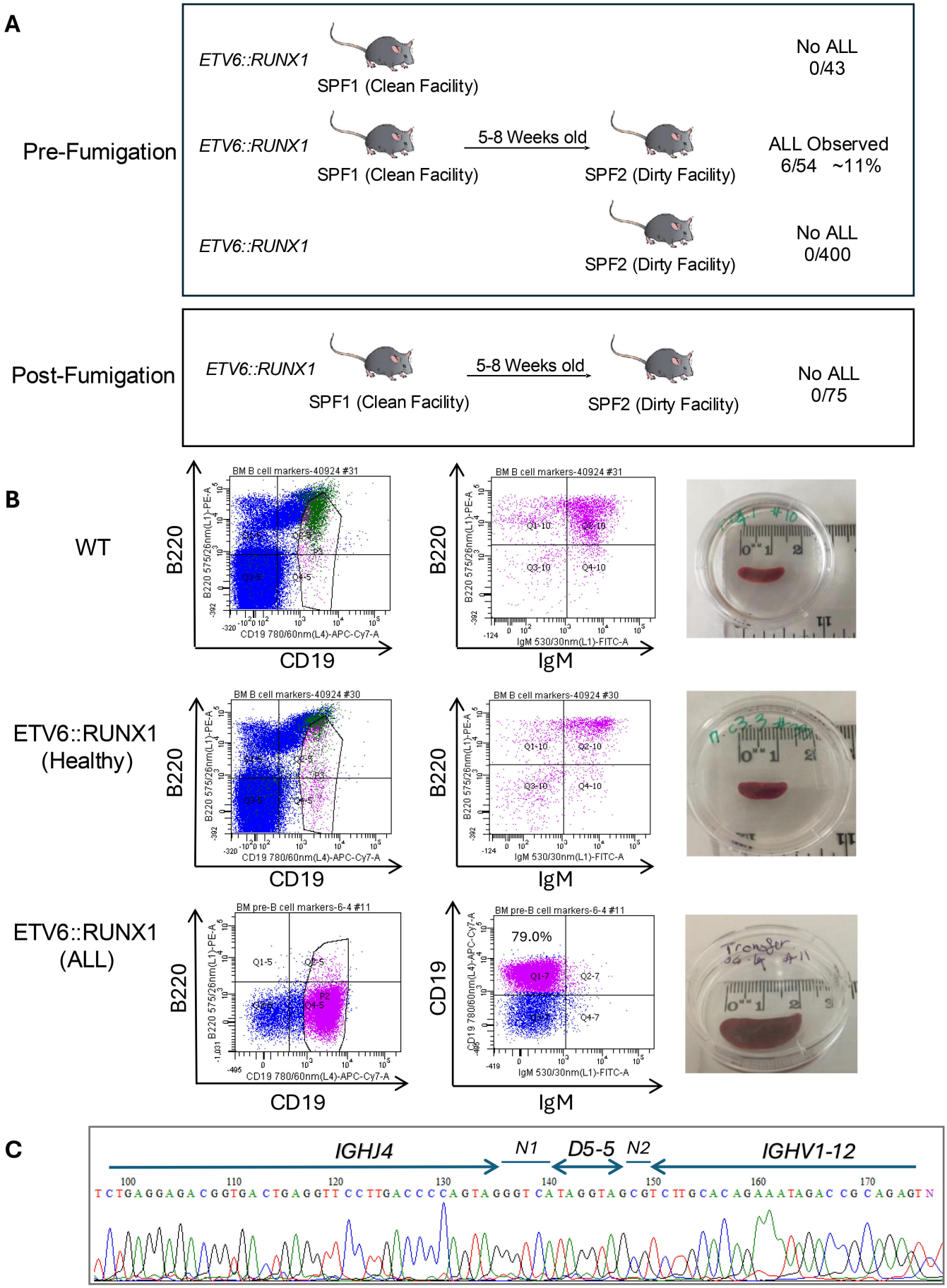
A
Pre-Fumigation
ETV6::RUNX1
SPF1 (Clean Facility)
No ALL
0/43
ETV6::RUNX1
SPF1 (Clean Facility)
5-8 Weeks old
SPF2 (Dirty Facility)
ALL Observed
6/54 ~11%
ETV6::RUNX1
SPF2 (Dirty Facility)
No ALL
0/400
Post-Fumigation
ETV6::RUNX1
SPF1 (Clean Facility)
5-8 Weeks old
SPF2 (Dirty Facility)
No ALL
0/75
B
WT
ETV6::RUNX1
(Healthy)
ETV6::RUNX1
(ALL)
BM B cell markers-40924 #31
BM B cell markers-40924 #30
BM pre-B cell markers-6-4 #11
B220
CD19
IgM
79.0%
C
IGHJ4
N1
D5-5
N2
IGHV1-12
TCTGAGGAGACGGTGACTGAGGTTCCTTGACCCCAGTAGGGTCATAGGTAGCGTCTTGCACAGAAATAGACCGCAGAGTN

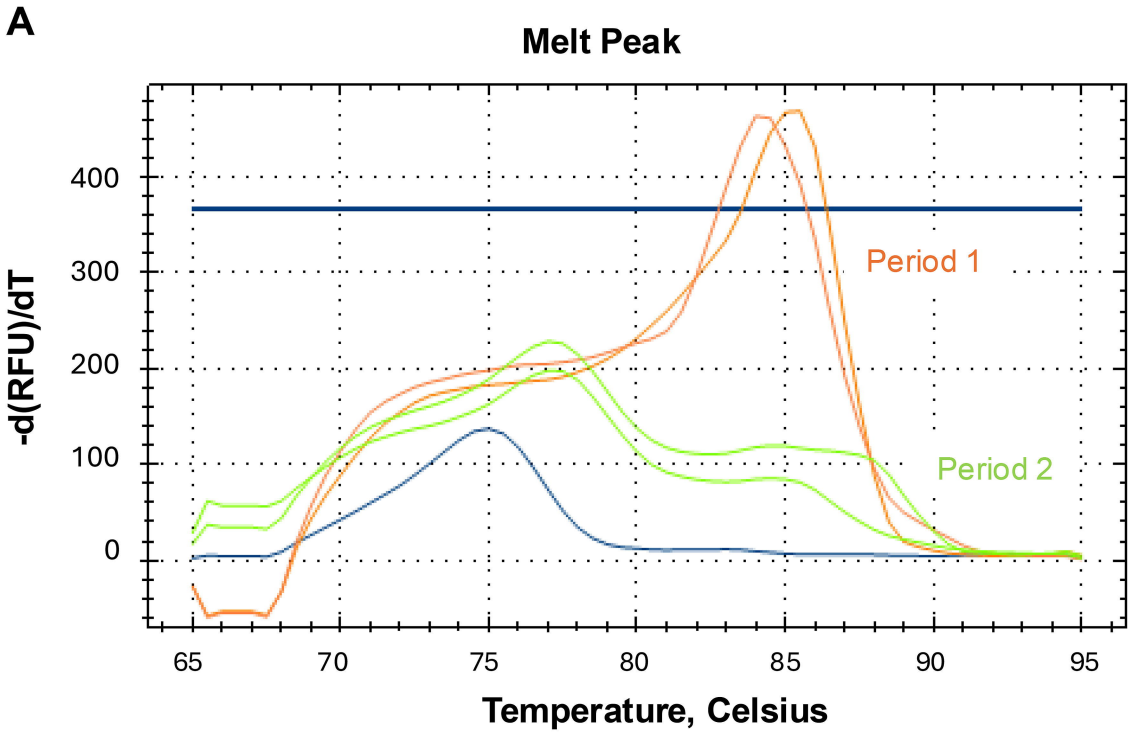
A
Melt Peak
-d(RFU)/dT
400
300
200
100
0
Period 1
Period 2
65
70
75
80
85
90
95
Temperature, Celsius

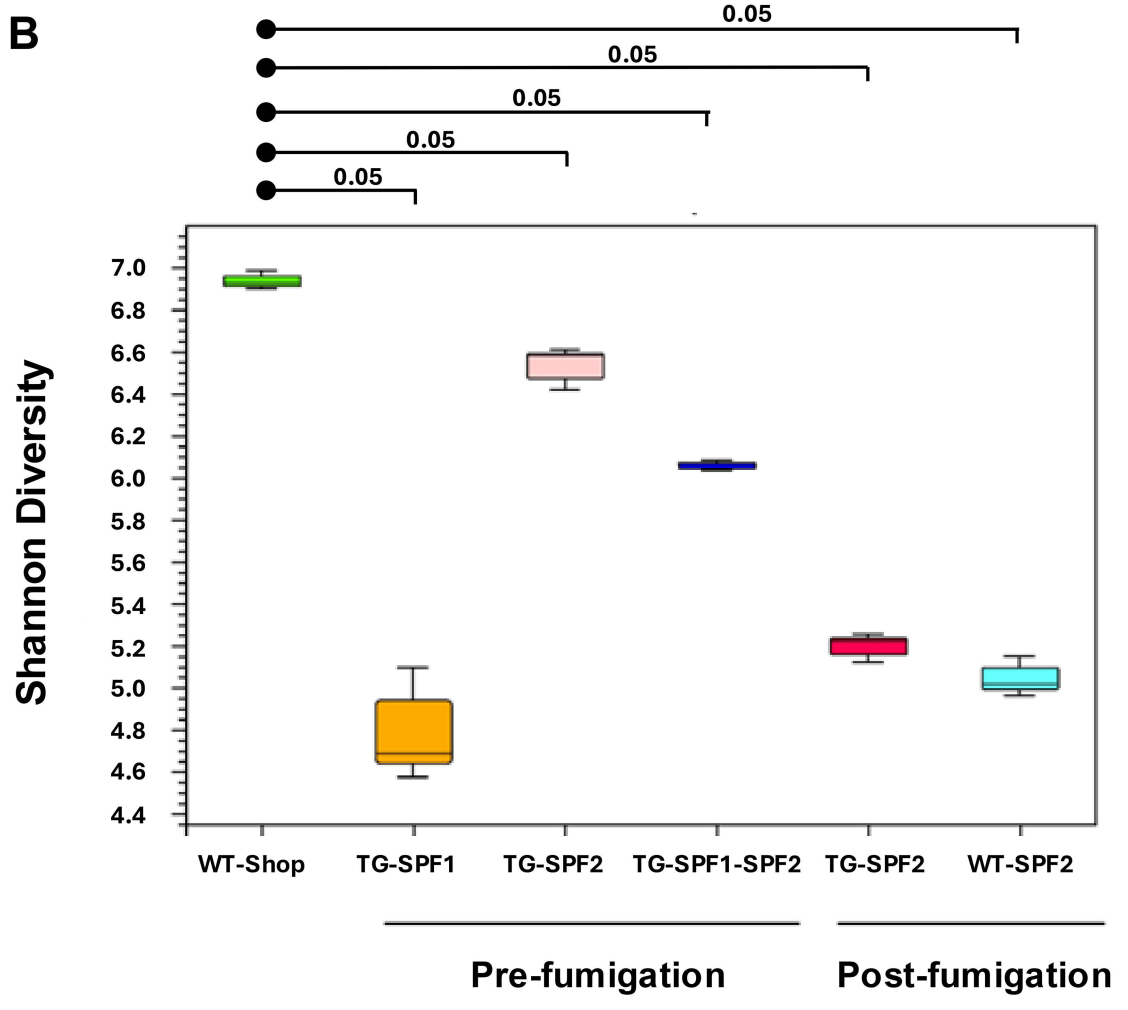
B
0.05
0.05
0.05
0.05
0.05
Shannon Diversity
7.0
6.8
6.6
6.4
6.2
6.0
5.8
5.6
5.4
5.2
5.0
4.8
4.6
4.4
WT-Shop
TG-SPF1
TG-SPF2
TG-SPF1-SPF2
TG-SPF2
WT-SPF2
Pre-fumigation
Post-fumigation

Supplementary Figures

Supplementary Figure 1

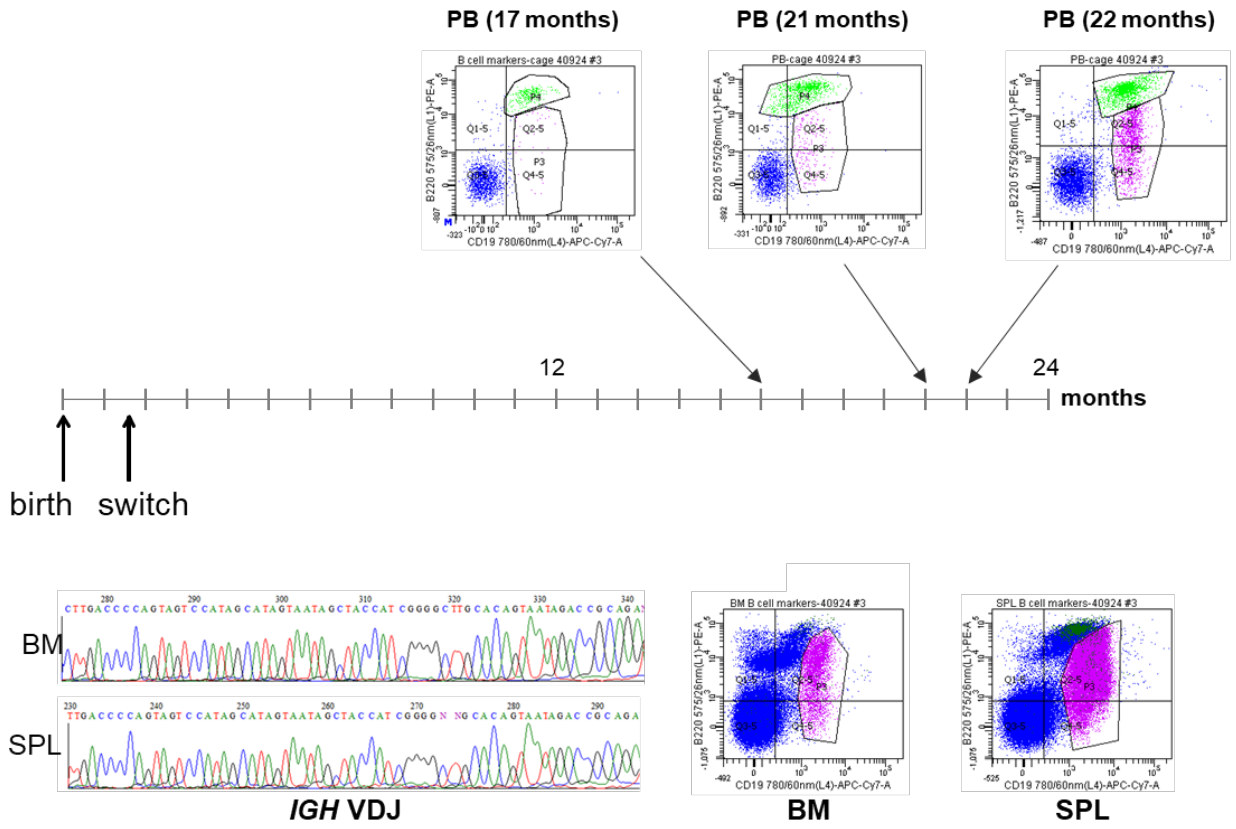

Emergence of the leukaemic clone

Temporal representation of periodic PB analysis of mice transferred from SPF1 to the SPF-2 facility.

Top: periodical immunophenotype analysis of PB showing (in a single mouse) the onset of the BCP-ALL clone at 17, 21 and 22 months of age.

Bottom: *IGH* VDJ DNA sequencing and immunophenotype analysis at experimental termination shows the presence of the same clone both in both bone marrow (BM) and spleen (SPL).

Supplementary Figure 2A

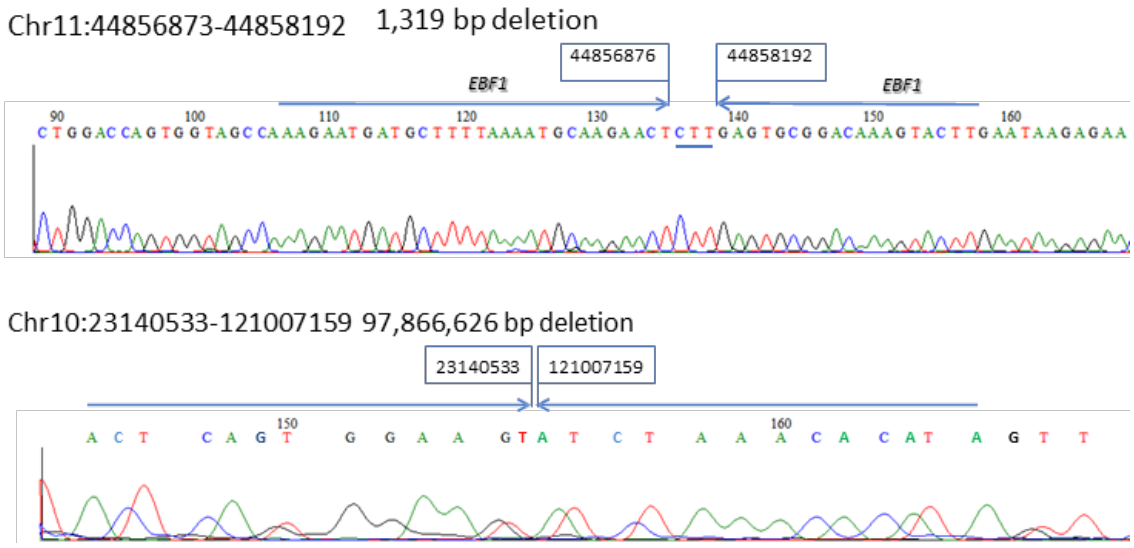

Genetic alterations identified by WGS. Top: 1319 bp deletion in *Ebf1* gene; Bottom: deletion in a large region of Chromosome10, including *Btg1* and *Arid5b* genes.

Supplementary Figure 2B

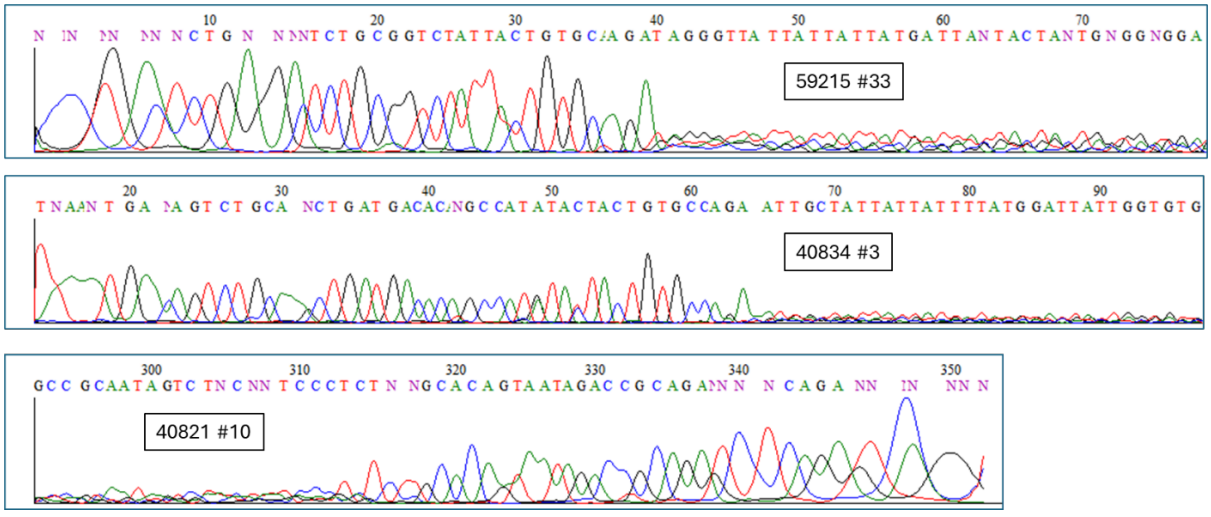

Polyclonal IGH gene rearrangements in typical examples of non-leukaemic mice born and maintained in SPF2 BEFORE fumigation of the facility.

Top Panel: primers C1 for VH J558 (PCR with JH4)
CGAGCTCTCCARCACAGCCTWCATGCARCTCARC

Middle panel: primers: C3 for VH 7183 (PCR with JH4)
CGGTACCAAGAASAMCCTGTWCCTGCAAATGASC

Bottom panel: C5 for VH J558 (PCR with JH4) CGGTACCAGACTGARCATCASCAAGGACAAYTCC

JH4 primer for PCR: CTGAGGAGACGGTGACTG AG

Supplementary Figure 3A

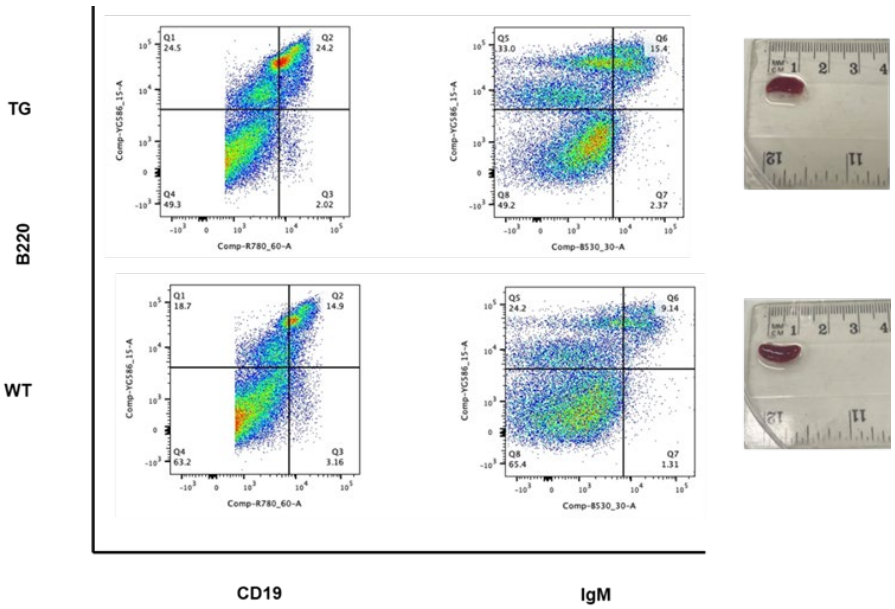

Polyclonal populations of BCP cells in examples of FACS profiles and spleens typical of non-leukaemic mice born in SPF1 and moved to SPF2 AFTER fumigation of the facility.

Supplementary Figure 3B

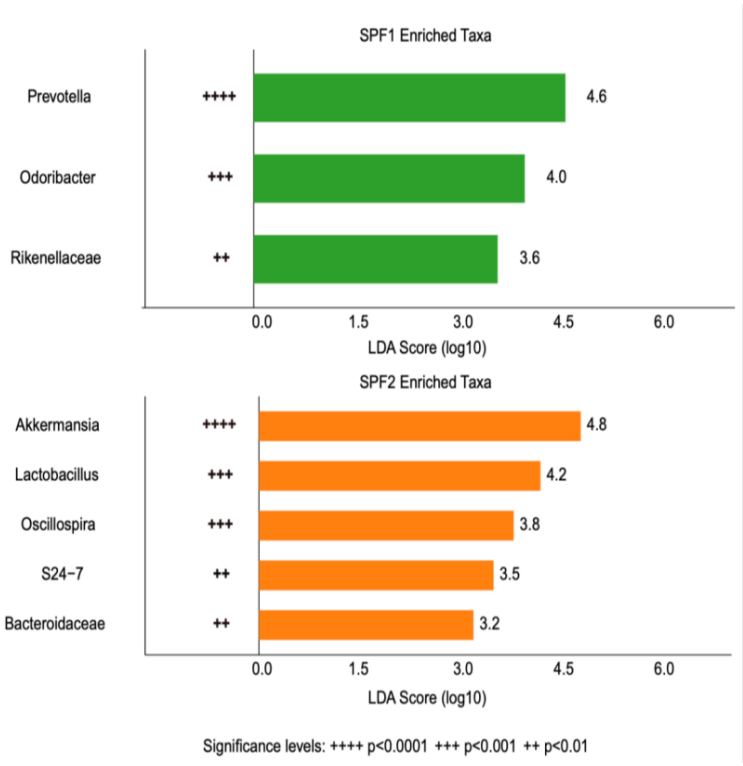

Linear Discriminant Analysis Effect Size (LEfSe) identifies different significantly enriched SCFA-producing bacterial taxa in SPF-1 (green) and SPF-2 (orange) housing environments. LDA scores (log10) reflect effect size.